Research Article | Vol. 28, No. 6 / 16 March 2020 / Optics Express 8658
Optics EXPRESS

Rotation-sensitive and direction-resolved homodyne laser-Doppler vibrometry method for simultaneous measurement of rotational and translational vibrations of a rigid object using a 1D array detector

SAIFOLLAH RASOULI[1,2,*] AND MOHAMMAD HOSSEIN DAEMI[1]

[1]Department of Physics, Institute for Advanced Studies in Basic Sciences, Zanjan 45137-66731, Iran
[2]Optics Research Center, Institute for Advanced Studies in Basic Sciences, Zanjan 45137-66731, Iran
*rasouli@iasbs.ac.ir

Abstract: In this paper, we introduce a new rotation-sensitive and direction-resolved homodyne laser-Doppler vibrometry method for rigid body vibration study that is based on the discrete Fourier-transform of successive 1D profiles of the moving interference fringes recorded with a 1D array detector. By investigating the temporal evolution of the spatial phase distribution of the 1D profiles of the interference fringes, the out-of-plane translational and rotational vibrations of the vibrating object are simultaneously determined. We use a direction-cosine-based approach to establish the theory of the measurements. The merits and limitations of the proposed method is described. We show that the proposed method can be used for detection of both tip and tilt changes and out-of-plane displacement measurements of a rigid body using a couple of parallel 1D array detectors. In addition, we show that the presented method can be also used on optical diffused surfaces by adding three lenses in a corner-like arrangement to the detecting system.

1. Introduction

Laser-Doppler Vibrometry (LDV) is an attracting method because of its non-contact, non-invasive, and remote action features. The signal from a typical homodyne LDV is insensitive to the motion direction [1]. Some techniques were used to overcome this deficiency [2,3,4]. We have recently employed two simple and low-cost methods based on the chasing of the straight-line interferometric fringes in order to give motion-direction-sensitivity to the homodyne LDV. In the first method, three point-detectors were used to extract the temporal-spatial phase of the interferometric fringes profile, using the spatial phase shift technique [5]. In the second method the chasing of the fringes were done by employing a 1D array detector to construct the *space-time image* which contain all the needed information to reconstruct the translational out-of-plane displacement of the object under the test [6].

On the other hand, in the surface profilometry of an object, if one produces a high-spatial-frequency fringe pattern, it is possible to reconstruct the surface profile of the object by a single-shot of the interference pattern without the need for temporal phase shift [7,8,9].

In this work, we introduce a modified homodyne LDV method that is capable of simultaneous measurement of the out-of-plane translational and rotational (including both tip and tilt angles) vibrations using a couple of parallel 1D array detectors. Theory of the work is presented using the direction cosines of the normal vector of the vibrating object and practical vibrometry results will be presented. We benefit discrete Fourier-transform (DFT) to extract the instantaneous 1D phase profiles of the interference fringes for the data of the 1D array detectors. We experimentally use the proposed method in the measurement of the out-of-plane translational and rotational (only tip angle) vibrations of a rigid body, using a single 1D array detector for simplicity. The

#384749 https://doi.org/10.1364/OE.384749
Journal © 2020 Received 29 Nov 2019; revised 30 Jan 2020; accepted 27 Feb 2020; published 11 Mar 2020

Optics EXPRESS

spatial-temporal phase profiles of the 1D array detector release the translational and rotational vibration waveforms, simultaneously.

It worth noting that one could measure the vibrations of a non-rigid body by employing a 2D sensor using simultaneous phase shifting techniques [10], but in such a case, the maximum measurable parameters of the vibration would be limited by the speed of the 2D array, which in general is lower than a 1D array.

2. Carrier pattern homodyne LDV

The temporal behavior of the intensity distribution in a well-aligned Michelson's interferometer (Fig. 1) represents contour fringes described by

$$I(x, y, t) = a(x, y) + b(x, y)\cos[\phi(x, y, t)], \tag{1}$$

where a and b are the DC level and modulation of the pattern, respectively. a and b are slowly varying functions of the position. ϕ is the phase lag of the measure beam relative to the reference beam. ϕ has generally position and time dependence that contain the translational and rotational information of the surface under the test. Because the cosine function is not a monotonic function, in general it is not possible to extract ϕ directly. Instead, if the reference mirror and test mirror (the body under the test) of the interferometer are tilted (say both the reference and measure beams experience tip/tilt angles) the corresponding beams will have oblique incidence on the observation plane. On the observation plane, k-vectors of the interfering beams can be written using their direction cosines:

$$\mathbf{k}_{r,m} = k\alpha_{r,m}\hat{\mathbf{x}} + k\beta_{r,m}\hat{\mathbf{y}} + k\gamma_{r,m}\hat{\mathbf{z}}, \tag{2}$$

where k shows the wavenumber of the laser beam, r and m denote reference and measure beams, α, β and γ show the direction cosines of the k-vectors corresponding to the $\hat{\mathbf{x}}$, $\hat{\mathbf{y}}$, and $\hat{\mathbf{z}}$ directions respectively (say $\alpha = \cos[\angle(\mathbf{k},\hat{\mathbf{x}})]$ and so forth). The interference pattern on the observation plane ($z = 0$ plane) can be calculated as

$$I(z = 0) = a + b\cos[k(\alpha_m - \alpha_r)x + k(\beta_m - \beta_r)y + \phi_{tr}], \tag{3}$$

where ϕ_{tr} shows a part of fringes' phase ϕ that is only originated from the translational displacement. To remove beam displacement on the observation plane due to angular deviation of the interfering beams, we employed a relay-imaging system to image both of the mirrors simultaneously on the observation plane (Fig. 1). The intensity distribution presented in Eq. (3) has high spatial frequencies $f_x = (\alpha_m - \alpha_r)/\lambda$ and $f_y = (\beta_m - \beta_r)/\lambda$ along x- and y-axis, respectively, which is modulated by the information function ϕ_{tr}, where λ is the wavelength of the beams. Here f_x depends only on α and not on β and similarly f_y depends only on β. Therefore, in the direction-cosine-based analysis, by choosing fixed values for α_r and β_r, the interference fringes period in the x- and y- directions directly release the direction cosines of the measure beam.

According to the reflection law and magnification property of the relay imaging system, in the paraxial approximation, the direction cosines of the vibrating object are related to the direction cosines of the measure beam at the observation plane by $\alpha_{\text{obj}} = \alpha_m M/2$ and $\beta_{\text{obj}} = \beta_m M/2$.

In practice, the use of 1D intensity profiles recorded by a 1D array detector(s) reduces instrument and process costs, remarkably. In the use of 1D array detector, to have the maximum spatial frequency of the fringes on the detector, fringes are tuned to be aligned almost perpendicular to the detector's array. In this scheme we consider array detector direction as y- axis.

Optics EXPRESS

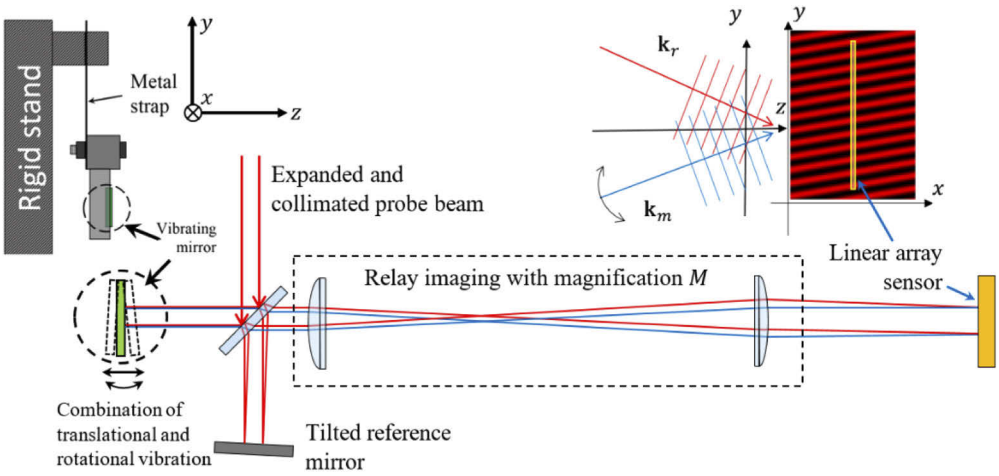

Fig. 1. Experimental setup for the measurement. The upper left inset shows the vibrating mirror (see Visualization 1).

Now let us rewrite Eq. (3) along a line parallel to y-axis, at $x = x_1$

$$I = a + b\cos(2\pi f_y y + \varphi),\ \varphi = 2\pi f_x x_1 + \phi_{tr}. \tag{4}$$

Taking Fourier transform of Eq. (4) leads to

$$\mathcal{F}(I) = \mathcal{F}(a) + \mathcal{F}(\frac{b}{2}e^{-i[2\pi f_y y+\varphi]}) + \mathcal{F}(\frac{b}{2}e^{i[2\pi f_y y+\varphi]}). \tag{5}$$

For an enough large value of f_y, three components of Eq. (5) are distant from each other in the Fourier domain. Isolating one of the side lobes of the frequency components, we calculate the total phase $2\pi f_y y + \varphi$ using inverse Fourier transform of it [7].

For a constant α_m, the time evolution of 1D intensity profile presented in Eq. (4) is enough for extraction of the out-of-plane translational vibration simultaneously with changes of the β_m. For such a case if $\alpha_m = 0$, the direction cosine β_m uniquely specifies the tilt angle of the measure beam θ_m, via relation $\sin\theta_m = \beta_m$, because the angles $\angle(\mathbf{k},\hat{\mathbf{y}})$ and θ_m are complementary angles. For small angular deviations, which is true for our cases (as will be shown in the following sections) we will replace the sine function with its argument. The tilt angle of the object will be $\theta_{\text{obj}} = \beta_m/2M$.

As a given frame of the 1D fringe profile has a constant spatial period, its phase has a linear function of y. During vibration of the object, y-intercept of this linear function determines the out-of-plane displacement of the object and its slope changes determine the time evolution of the direction cosine β_m of the measure beam. Besides, a change in the direction cosine α_m leads to a change in f_x, which is equivalent to the rotation of the fringes. With the aid of two 1D array detectors implemented parallel to each other, it is possible to determine direction cosine α_m (See Visualization 1).

Using temporal evolution of the phase values detected by the detectors at a given altitude y, we determine temporal evolution of the fringes direction. Evolution the fringes direction releases evolutions the fringes period in the x-direction and f_x (see Fig. 2):

$$\frac{d}{dt}\Lambda_x = \Lambda_y\frac{d}{dt}(\tan\theta_F) = \frac{\Lambda^2{}_y}{2\pi d}\frac{d}{dt}(\varphi_{D_2} - \varphi_{D_1}), \tag{6}$$

Optics EXPRESS

where φ_{D_1} and φ_{D_2} are the extracted phase values by the sensors at the given altitude. Using temporal evolution of Λ_x, the temporal evolution of the corresponding direction cosine α_m, and the orientation of the object will be declared.

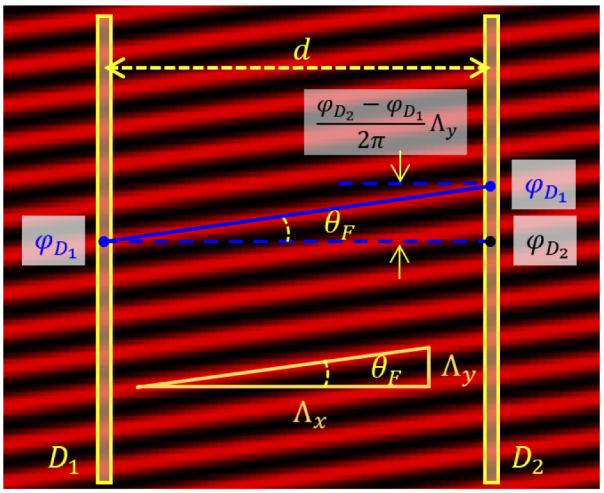

Fig. 2. Employing two parallel 1D sensors to extract the fringes angle.

3. Experimental implementation

Using the proposed homodyne LDV method, we measured vibrations of a flat mirror attached to one end of a metal strap (upper-left inset of Fig. 1). Neglecting the changes of the direction cosine α, the general motion of the mirror can be considered in two dimensions and can be decomposed to a translational motion of its center relative to a reference frame and a rotational motion around its center. We used a linear array sensor, TSL1402R from TAOS along y-direction for capturing the instantaneous fringe profiles. This sensor has 256 pixels of size 63.5 µm × 55.5 µm with 63.5 µm spacing between the centers of the adjacent pixels (16.25 mm of total length). The driver of the sensor can yield maximum sampling rate of R_L = 19157 line/sec. Due to the suspended form of the mirror mounting, the fringe displacements are mainly in the vertical direction. Using the proposed method, we measured the impulse response and the reaction of the system to air blowing. The procedure of extracting the motion of the mirror is demonstrated in Fig. 3 (see also Visualization 2). During the vibration, we saved the 1D fringe profiles in a computer. By sewing successive 1D fringes profiles, we obtain a space-time image (STI) that contains all the mirror vibration information. We applied the DFT analysis to each column of the STI and extracted corresponding phase profiles. In the discrete Fourier transform of the 1D data, to get rid of the edge artifacts, after transforming procedure we cut 19 pixels from each ends of the resulted phase profiles. The motion of the mirror is calculated using 2D phase profile of the STI that is a wavy slanted surface. Along space coordinate, it has a mean slope and along time coordinate, it shows an oscillating behavior. After removing mean slant of the STI phase profile, as the motion is a combination of the translational and rotational vibrations, the instantaneous slope of the resulted phase profile along space coordinate determines angular changes of the measure direction cosine, β_m. The mean value of the 1D phase profile yields the instantaneous out-of-plane displacement after applying a transformation factor of $\lambda/4\pi M$. The spectra of the translational and rotational vibrations are demonstrated in Fig. 4.

Optics EXPRESS

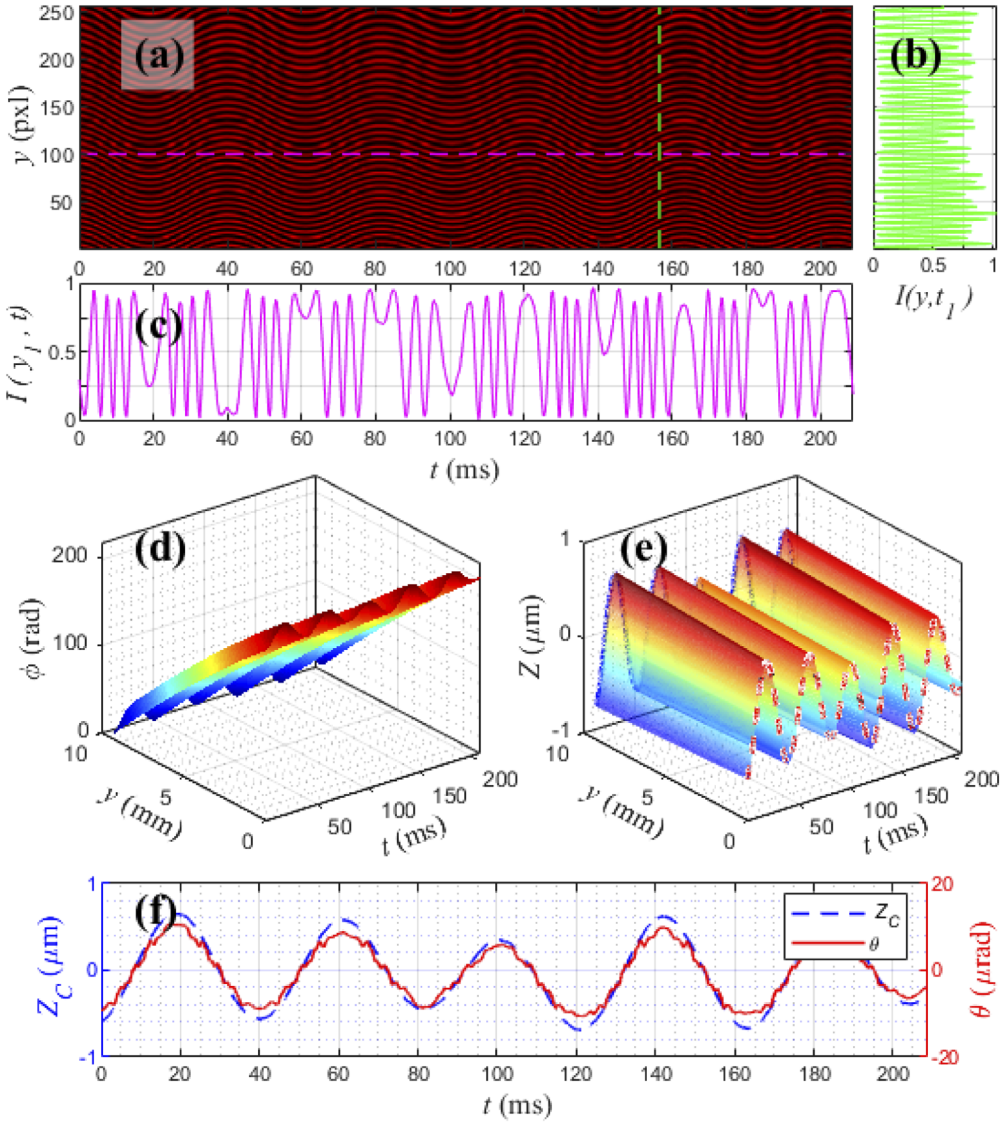

Fig. 3. (a) Recorded space-time image of the 1D fringe-profile during mirror vibration. (b) Fringe profile at a give frame correspoding to the vertical dashed line in (a). (c) Homodyne signal recorded by the pixel No. 100 of the sensor depicted by a horizontal dashed line in magenta color in (a). (d) The extracted phase from the Fourier analysis. The periodic form of the profile imposes a mean slant to the reconstructed phase. (e) shows the displacements of a measuring line on the vibrating mirror by removing the average slant fom (d) and applying the transformation factor. (f) demonstrates the displacements of central point of the measuring line and calculated changes of the miror tilt (see Visualization 2).

Optics EXPRESS

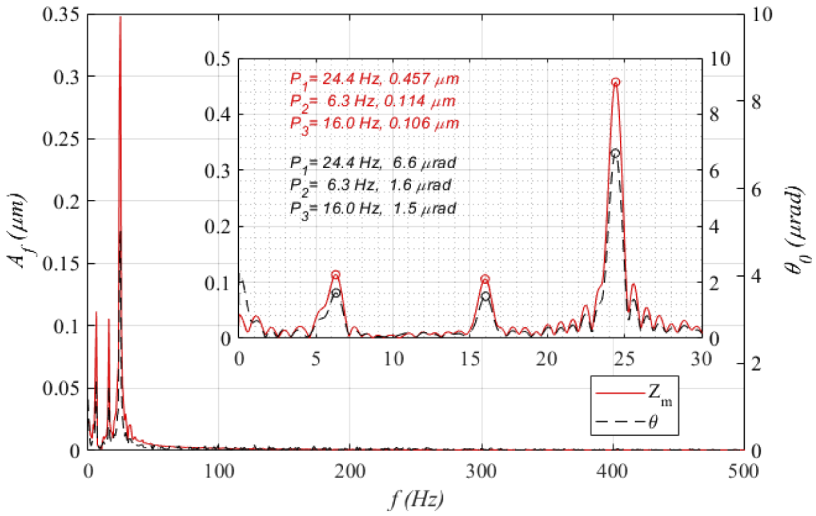

Fig. 4. The typical spectrum of the translational and rotational vibrations of the mirror. The inset shows the spectra in a closer view. Because of spectral leakage of DFT, the locations of the spectrum peaks and their heights may differ from the actual values. In order to extract the peaks location and height, a 32 times zero-padding DFT is used for extraction of the vibration parameters. Due to the specific structure of the vibrational system (pendulum-like), the spectra of the rotational and translational vibrations are correlated.

4. Limitations

Limitedness of the spatial resolution and number of pixels (N) of the array sensor and its data acquisition rate will limit the measuring capability of the method. On the other hand, the intensity signal detected by a pixel of the array sensor is a homodyne signal, which is typically a chirped signal (see Fig. 3(c)). If the analogue bandwidth of the instrument is not wide enough the transmitted electrical signal will be deformed and the peak-to-valley (PV) of the homodyne intensity signal will decrease in the regions that the temporal frequency is high. Effect of the limited bandwidth of the transmission line on a homodyne signal is typically demonstrated in Fig. 5. This may lead to errors on the extraction of the vibrational parameters. In the case of pure translational vibration, all of the pixels of the sensor experiences the same intensity variations so the PV of the profile will change as time for all of the pixels in a same manner. In this case, the low bandwidth will limit the bit-depth of the recorded spatial profile, which subsequently will limit the resolution of the measurement. For a high-amplitude rotational vibration, this limitedness leads to an amplitude modulation of the detected profile, because the temporal intensity variations differ for different pixels. Pixels near to the point conjugate to the vibration axis, experience lower intensity changes and pixels far from it experience more rapid intensity changes. Albeit based on the following calculations, for the used array sensor the maximum measurable vibration amplitude, mainly limited by the spatial specifications and sampling rate of the sensor. The sensor can operate up to 8 MHz (compare with R_L<20 kHz of the sampling rate), which indicates that the analogue bandwidth is not at all a limiting parameter.

Here we describe how the spatial specifications and sampling rate determine the measurable vibration parameters. In order to calculate the capability borders of the proposed method, we consider again a flat reflecting mirror with a general two-dimensional motion. The fringe pattern lines are considered perpendicular to the array direction. Spatial resolution and number of pixels of the sensor are the determinant factors to sense the periodicity of the carrier pattern. The minimum measurable spatial frequency is zero. However, in order to implement the proposed

Optics EXPRESS

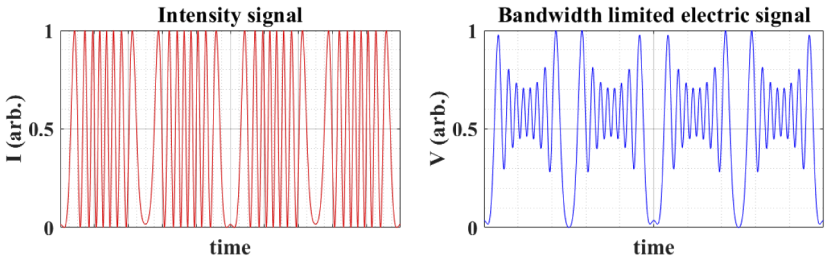

Fig. 5. (Left) A typical chirped homodyne signal of a vibration with an amplitude of $A = 2\lambda$. (Right) The detected signal with a band-limited detection system.

method via isolating the one of the side frequency components of the DFT, the recorded data should covers at least two periods of the fringe pattern. On the other hand, the highest value for the spatial frequency is determined by the Nyquist's criterion. Therefore, with δy as the inter-pixel distance, the range of spatial frequencies in DFT will be

$$f_y = \frac{2}{N\delta y} : \frac{1}{N\delta y} : \frac{N/2-1}{N\delta y}. \tag{7}$$

Total frequency span, Δf_y and mean value, $\overline{f_y}$ are accordingly

$$\Delta f_y = \frac{1}{\delta y}\left(\frac{1}{2} - \frac{3}{N}\right), \overline{f_y} = \frac{1}{\delta y}\left(\frac{1}{4} + \frac{1}{2N}\right). \tag{8}$$

In order to utilize all of the potential of the instrument for measuring the angular vibration, one should tune the angle of the reference mirror to a value that in the equilibrium angle of the vibrating object, the produced spatial frequency be $f_y = \overline{f_y}$. In this case, the maximum angular deviation of the vibrating object will be in the range $\pm\Delta f_y/2$. Therefore the maximum measurable direction cosine $\beta_{\text{obj, max}}$ is

$$\beta_{\text{obj.,max}} = M\lambda/4 \times \Delta f_y, \tag{9}$$

which is accessible when the direction cosine of the reference mirror $\beta_{\text{ref. mirror}}$ is tunes to an amount of

$$\beta_{\text{ref. mirror}} = M\lambda/2 \times \overline{f_y}. \tag{10}$$

In our case with $M = -1.5$ and $\lambda = 0.633$ µm and considering $N = 256$ and $\delta y = 63.5$ µm of the sensor, the maximum measurable amplitude for angular vibration is $\beta_{\text{obj, max}} = 1.825 \times 10^{-3}$, with $\beta_{\text{ref. mirror}} = 1.884 \times 10^{-3}$.

Now we determine limitations caused by the finite sampling rate. In the time interval between two successive line capturing, the phase change in any point of the measurement region should not exceed π radian, otherwise, the phase continuity will be spoiled. This means that the maximum out-of-plane displacement of any point on the vibrating object should not exceed $Z_{\text{max}} = M\lambda/4$ in the time interval between two successive sampling times $\delta t = 1/R_L$. For the considered two-dimensional motion, the maximum displacement during δt occurs at one of the either ends of the measuring line that is given by

$$Z_{\text{max}} = Z_{\text{C, max}} + \ell\beta_{\text{obj, max}}/2, \tag{11}$$

with $Z_{\text{C, max}}$ as the maximum displacement of the center of the measuring line. ℓ is the length of the measuring line and $\beta_{\text{obj, max}}$ is maximum angular deviation of the object around its center. Maximum displacement occurs when the measuring time span is centered at a quadrature point

Optics EXPRESS

(a point with maximum velocity). Using this fact the maximum translational and rotational displacement for corresponding harmonic vibrations in a time interval of $\delta t = 1/R_L$ are as below:

$$\begin{aligned} Z_{\mathrm{C,\ max}} &= Z(\mathrm{t} = \tfrac{1}{2\mathrm{R}_L}) - Z(\mathrm{t} = \tfrac{-1}{2\mathrm{R}_L}) = 2A\sin(\tfrac{\pi f_{\mathrm{tr}}}{R_L}), \\ \beta_{\mathrm{obj,\ max}} &= \beta_{\mathrm{obj}}(\mathrm{t} = \tfrac{1}{2\mathrm{R}_L}) - \beta_{\mathrm{obj}}(\mathrm{t} = \tfrac{-1}{2\mathrm{R}_L}) = 2\beta_{\mathrm{obj,0}}\sin(\tfrac{\pi f_{\mathrm{rot}}}{R_L}), \end{aligned} \tag{12}$$

with A and $\beta_{\mathrm{obj,0}}$ as the amplitude of the translational and direction cosine β_{obj} vibrations, respectively. Likewise, f_{tr} and f_{rot} are corresponding vibration frequencies. Therefore, Eq. (12) can be written as

$$Z_{\max} = \frac{M\lambda}{4} \Rightarrow A\sin\left(\frac{\pi f_{\mathrm{tr}}}{R_L}\right) + \frac{\ell}{2}\beta_{\mathrm{obj,0}}\sin\left(\frac{\pi f_{\mathrm{rot}}}{R_L}\right) = \frac{M\lambda}{8}. \tag{13}$$

In the case of independent translational and rotational vibrations, for given values of f_{tr} and f_{rot}, the maximum measurable values for amplitudes A and $\beta_{\mathrm{obj,0}}$ should satisfy Eq. (13). This equation with the fact that f_{tr}, $f_{rot} \leq 2/R_L$ (Nyquist's criterion), determines the measurable parameters of a two-dimensional vibration. In many practical cases, the translational and rotational vibrations have the same frequency, f (e.g. for a rigid object with a rotational vibration around an axis that resides outside of the measurement region). In such a case, Eq. (13) will have a simpler form of

$$A + \frac{\ell}{2}\beta_{\mathrm{obj}} = \frac{M\lambda}{8\sin(\pi f/R_L)}. \tag{14}$$

The magnification M expands the applicable region in the expense of reducing the size of the measurement line.

5. Additional discussion: vibrometry of a non-mirror solid object

The method described above, is useable for vibrometry of a solid object having polished surface in which it can be considered as a flat mirror that we call it "mirror-like surface". A vibrating mirror-like surface will not affect the form of the wavefront of the measure beam, and only approximately reverses its Poynting vector and changes its overall phase. The above-presented method is not usable for a non-mirror-like vibrating surface. Nevertheless, it is known that by inserting a lens in front of such a non-mirror-like vibrating object, one can produce a nearly flat wavefront of the beam after reflection from the object and retransmitting it through the lens. The only requirement is the object surface should has a reasonable reflection toward the inserted lens. The relay imaging system must be tuned to image the inserted lens on the detector. We previously used this technique to overcome the effect of the local curvature of the object under the test [6]. However, in such a circumstance, the system will detect only the translational vibration, and the rotational vibration has no effect on the fringes pattern. For simultaneous measurement of the translational out-of-plane and rotational vibrations of a non-mirror-like solid object, we propose a modification to the system described in the previous sections. By inserting three lenses in a corner-like arrangement instead of a single lens, one can produce three focus spots on the surface of the vibrating object (see Fig. 6). Now there were be three measure beams that their respective phase delays are governed by the spatial locations of the lenses and the out-of-plane displacement of the object at the focal points. Two vertical lenslets produce two interference patterns vertically that can be recorded using a single 1D array detector. These patterns are analyzed separately; the evolution of each pattern declares the out-of-plane translational motion of the object at the corresponding points. By comparing the displacements at these two points, the β direction cosine can be calculated. Comparing patterns of two horizontal lenses, one can extract the temporal evolution of the α direction cosine, too. For analyzing of the patterns, one can use the method described in this paper, or by fringe tracing method [6,11].

Optics EXPRESS

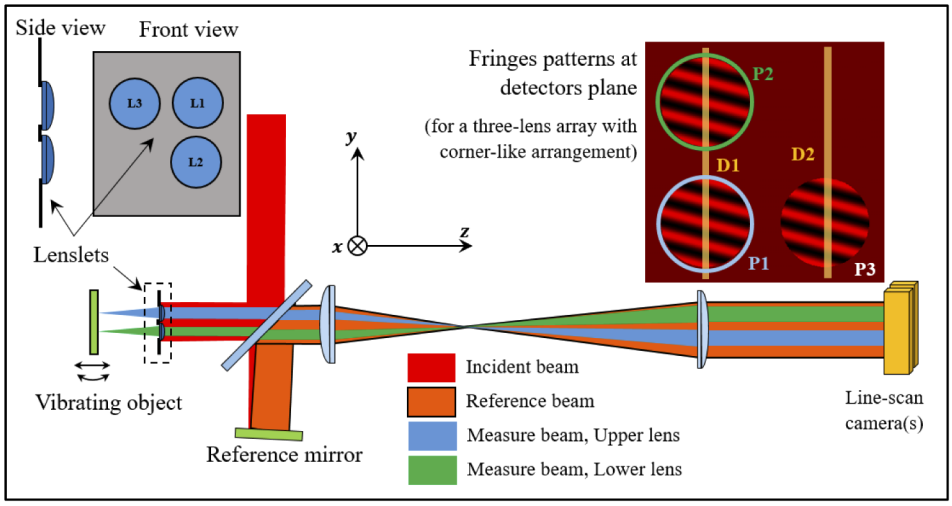

Fig. 6. The use of three-lens array in the proposed method for simultaneous measurement of the translational and rotational vibrations of a non-mirror-like object. A set of three lenses (or micro-lenses) form a corner-like array used in the path of measure beam close to the vibrating object. Two lenses located in the vertical direction shown in the setup (**L1** and **L2**) produce two measure beams which are depicted with different colors for the ease of demonstration. The patterns at the detector(s) plane are shown in the upper-right inset figure. Patterns **P1**, **P2** and **P3** are produced by interfering of the beams passed through the lenses L1, L2 and L3, respectively with the reference beam. The translational displacements and β direction cosine can be calculated from the patterns on a single detector **D1**, if the patterns analyzed separately using the Fourier analysis or space-time fringes method. Using the third lens (**L3**) and producing the pattern P3 on the second detector **D2**, the displacement data for the third point is calculated. Comparing these data with the date of lens L1, one can declare the α direction cosine with the similar analysis described in the previous sections.

6. Conclusion

A rotation-sensitive and direction-resolved homodyne laser-Doppler vibrometry method was introduced for rigid body vibration study. We used a direction-cosine-based approach to establish the theory of the measurements. The conventional LDV method abled rotation- and direction-sensitivity just by using a 1D array detector, therefore this modification of the LDV setup is simple and low-cost. In practice, with the aid of a 1D array sensor, we measured motion of a line on a mirror attached to a mechanical oscillator. Using discrete Fourier-transform of moving fringes' profiles, we measured simultaneously the translational and rotational vibrations of the vibrating line. The potential effect of the limited transmission bandwidth of the instrument was discussed. For our case, the bandwidth of the instrument is adequate and is not a limiting factor. The limitations of the method are practically due to spatial specifications of the sensor and sampling rate of the driver, which both of them were investigated in detail. The proposed method can be experimentally applied for the study of three-dimensional vibration of a rigid body with the aid of only two 1D detectors.

The method was described for the case that the object is a polished, flat, and reflective surface. In order to implement the presented method on a non-mirror-like object such as optical diffused surfaces, a modification to the optical setup was proposed using a three lenses array.

Optics EXPRESS

Disclosures

The authors declare no conflicts of interest.

References

1. H. -E. Albrecht, M. Borys, N. Damaschke, and C. Tropea, *Laser Doppler and Phase Doppler Measurement Techniques*, Springer, 2002.
2. F. J. Eberhardt and F. A. Andrews, "Laser Heterodyne System for Measurement and Analysis of Vibration," J. Acoust. Soc. Am. **48**(3A), 603–609 (1970).
3. D. Jackson, A. Kersey, M. Corke, and J. Jones, "Pseudoheterodyne detection scheme for optical interferometers," Electron. Lett. **18**(25-26), 1081–1083 (1982).
4. S. Rerucha, Z. Buchta, M. Sarbort, J. Lazar, and O. Cip, "Detection of Interference Phase by Digital Computation of Quadrature Signals in Homodyne Laser Interferometry," Sensors **12**(10), 14095–14112 (2012).
5. M. H. Daemi and S. Rasouli, "Fringe chasing by three-point spatial phase shifting for discrimination of the motion direction in the long-range homodyne laser Doppler vibrometry," Opt. Laser Technol. **103**, 387–395 (2018).
6. M. H. Daemi and S. Rasouli, "Direction-resolved homodyne laser-Doppler vibrometry by analyzing space-time fringes created by the successive 1D intensity profiles of the interference fringes," Opt. Lett. **44**(23), 5824–5827 (2019).
7. M. Takeda, H. Ina, and S. Kobayashi, "Fourier-transform method of fringe-pattern analysis for computer-basedtopography and interferometry," J. Opt. Soc. Am. **72**(1), 156–160 (1982).
8. T. Ikeda, "Hilbert phase microscopy for investigating fast dynamic in transparent systems," Opt. Lett. **30**(10), 1165–1167 (2005).
9. M. R. Jafarfard, M. H. Daemi, and S. Kazemi, "Online measurement of the optical aberrations of a thin-disk laser active medium using the Fourier domain multiplexing method," J. Opt. Soc. Am. B **36**(10), 2884–2888 (2019).
10. N. Brock, J. Hayes, B. Kimbrough, J. Millerd, M. North-Morris, M. Novak, and J. C. Wyant, "Dynamic Interferometry," Proc. SPIE **5875**, 58750F (2005).
11. S. Rasouli and M. Shahmohammadi, "Portable and long-range displacement and vibration sensor that chases moving moiré fringes using the three-point intensity detection method," OSA Continuum **1**(3), 1012–1025 (2018).